



STANDARD ARTICLE

In vivo detection of microstructural spinal cord lesions in dogs with degenerative myelopathy using diffusion tensor imaging

Philippa J. Johnson¹  | Andrew D. Miller² | Jonathan Cheetham¹ |
 Elena A. Demeter² | Wen-Ming Luh³ | John P. Loftus¹  | Sarah L. Stephan¹ |
 Curtis W. Dewey¹ | Erica F. Barry¹

¹Department of Clinical Sciences, Cornell College of Veterinary Medicine, Cornell University, Ithaca, New York

²Department of Biomedical Sciences, Cornell College of Veterinary Medicine, Cornell University, Ithaca, New York

³National Institute on Aging, National Institutes of Health, Bethesda, Maryland

Correspondence

Philippa J. Johnson, Department of Clinical Sciences, College of Veterinary Medicine, Cornell University, 930 Campus Road, Ithaca, NY 14853.

Email: pjj43@cornell.edu

Funding information

Morris Animal Foundation, Grant/Award Number: D18CA-310

Abstract

Background: Degenerative myelopathy (DM) in dogs is a progressive neurodegenerative condition that causes white matter spinal cord lesions. These lesions are undetectable on standard magnetic resonance imaging (MRI), limiting diagnosis and monitoring of the disease. Spinal cord lesions cause disruption to the structural integrity of the axons causing water diffusion to become more random and less anisotropic. These changes are detectable by the technique of diffusion tensor imaging (DTI) which is highly sensitive to diffusion alterations secondary to white matter lesion development.

Objective: Perform spinal DTI on cohorts of dogs with and without DM to identify if lesions caused by DM will cause a detectable alteration in spinal cord diffusivity that correlates with neurological status.

Animals: Thirteen dogs with DM and 13 aged-matched controls.

Methods: All animals underwent MRI with DTI of the entire spine. Diffusivity parameters fractional anisotropy (FA) and mean diffusivity (MD) were measured at each vertebral level and statistically compared between groups.

Results: Dogs with DM had significant decreases in FA within the regions of the spinal cord that had high expected lesion load. Decreases in FA were most significant in dogs with severe forms of the disease and correlated with neurological grade.

Conclusions and Clinical Importance: Findings suggest that FA has the potential to be a biomarker for spinal cord lesion development in DM and could play an important role in improving diagnosis and monitoring of this condition.

KEYWORDS

diffusion tensor imaging, fractional anisotropy, magnetic resonance imaging, mean diffusivity

Abbreviations: AD, axial diffusivity; ALS, amyotrophic lateral sclerosis; ASA, American Society of Anesthesiologists; CSF, cerebrospinal fluid; DICOM, Digital Imaging and Communications in Medicine; DM, degenerative myelopathy; DTI, diffusion tensor imaging; FA, fractional anisotropy; FDT, FMRIB Diffusion Toolkit; FOV, field of view; FS, female spayed; FSL, FMRIB's Software Library; GSD, German shepherd dog; IVDD, intervertebral disc disease; MD, mean diffusivity; MN, male neutered; MRI, magnetic resonance imaging; NIFTI, Neuroimaging Informatics Technology Initiative; NS, not sampled; PCA, principle component analysis; PD, proton density; PM, postmortem; RD, radial diffusivity; ROI, region of interest; SOD1, superoxide dismutase 1.

1 | INTRODUCTION

Degenerative myelopathy (DM) in dogs is a progressive neurodegenerative condition with a prevalence of 0.19% in pure and mixed breed dogs.¹ Middle to older aged dogs present with upper motor neuron signs of

This is an open access article under the terms of the Creative Commons Attribution-NonCommercial License, which permits use, distribution and reproduction in any medium, provided the original work is properly cited and is not used for commercial purposes.

© 2020 The Authors. *Journal of Veterinary Internal Medicine* published by Wiley Periodicals LLC, on behalf of the American College of Veterinary Internal Medicine.

asymmetric pelvic limb proprioceptive ataxia and progress to lower motor neuron paraplegia and eventually flaccid tetraplegia. This condition has no effective treatment and the resultant neurological dysfunction necessitates euthanasia.²

Currently, DM is only definitively diagnosed postmortem by histopathological examination of the spinal cord. Antemortem diagnosis is limited because the lesions are not visible on conventional magnetic resonance imaging (MRI) sequences and cerebrospinal fluid changes are not specific for DM.³ The disease is associated with a genetic mutation in superoxide dismutase 1 (SOD1). Dogs with DM are homozygous for the A allele of a SOD1 missense mutation and develop progressive axonal loss, demyelination and astrocytosis within the white matter of the major spinal cord funiculi,³ but not all dogs with the mutation develop DM.⁴⁻⁶ Clinical diagnosis of DM is therefore presumptive and made by excluding other causes for the clinical presentation and identifying a homozygous A allele SOD1 mutation.³ Developing an MRI method sensitive for DM-associated spinal cord lesions would be valuable for in vivo noninvasive diagnosis and provide a biomarker for noninvasive monitoring of lesion development throughout the lifetime of an affected dog.

In cohorts of humans with amyotrophic lateral sclerosis (ALS), a disease analogous to DM in dogs,^{7,8} diffusion tensor imaging (DTI) has reliably identified diffusivity alterations within the spinal cord that correlate with neurological dysfunction.⁸⁻¹⁰ Diffusion tensor imaging is an advanced MRI method that measures and quantifies the type of water diffusion within neurological tissue.¹¹⁻¹³ The degree of diffusion anisotropy in a voxel is documented by the parameter fractional anisotropy (FA), and the average diffusion within a voxel is documented by the parameter mean diffusivity (MD).^{12,14,15} Spinal cord white matter exhibits a characteristic pattern of water diffusion because the axons constrain water resulting in high FA and moderate MD values. When white matter is compromised, water diffusion becomes more random and less anisotropic. As such, when white matter lesions are present, FA values decrease and MD values are altered.¹⁶ Diffusion tensor imaging has been described and optimized in the normal canine spinal cord,^{15,17} and changes in FA have been identified in various spinal cord lesions.¹⁸⁻²⁰ This technique has the potential to sensitively detect white matter lesions within the spinal cord of dogs with DM, improving ability to monitor and diagnose the disease.

In this study we used DTI to evaluate the spinal cord of a cohort of dogs with DM. We aimed to evaluate the pattern of diffusivity alteration present in diseased spinal cords and correlate these changes to histopathology and expected lesion load. We aimed to test the hypothesis that diffusivity parameters will be significantly altered in the spinal cords of dogs with DM and that the pattern of these changes will correspond with expected lesion load within the spinal cord. We further hypothesized that the severity of diffusivity alterations will correlate with the neurological status of dogs with DM.

2 | MATERIALS AND METHODS

2.1 | DM cohort subject selection

Dogs for the DM cohort were recruited from a client-owned clinical population. The DM group candidates were included if they had

neurological signs of progressive, nonpainful T3-L3 localized neurological deterioration consistent with a diagnosis of DM, as determined by a board-certified veterinary neurologist. On genetic testing they were required to be homozygous for the A allele mutation (AA) at the SOD1 locus. In addition, for inclusion, imaging and necropsy results, when available, were required to exclude the presence of concurrent disease processes that could have contributed to the neurological status of each subject. All included subjects were required to have an American Society of Anesthesiologists (ASA) score < 2 after physical examinations and preanesthetic blood analysis.

2.2 | Control cohort subject selection

Dogs for the control cohort were recruited from research and client-owned populations. Dogs were required to be >8 years of age, > 5 kg in weight, and be neurologically normal and clinically healthy. All included subjects were required to have an ASA score < 2 after physical examinations and preanesthetic blood analysis. Only dogs with a negative (GG) result on SOD1 genetic testing were included in the control cohort. This study had approval from Cornell University's Institutional Animal Care and Use Committee.

2.3 | Neurological grading

All included subjects underwent full neurological examination and were graded according to a 15-point motor scale adapted from a scoring system for monitoring pelvic limb function as a result of thoracolumbar myelopathies (Table 1).²¹ Subjects in the DM cohort that had a neurological grade of 1 to 7 were placed in the mild DM group and dogs with a neurological grade of 8 to 14 were placed in the severe DM group. Subjects in the control cohorts that were not grade 0 were excluded from the study.

2.4 | Anesthesia

Dogs were imaged under general anesthesia performed by a board-certified veterinary anesthesiologist. All subjects were premedicated with dexmedetomidine (3 µg/kg; Dexdomitor, 0.5 mg/mL; Zoetis Inc, Kalamazoo, MI), induced to general anesthesia using propofol to effect (3.2-5.4 mg/kg; Sagent Pharmaceuticals, Schaumburg, Ill) and intubated. They were maintained under anesthesia using inhalant isoflurane and oxygen with a dexmedetomidine continuous rate infusion (1 µg/kg/hr Dexdomitor, 0.5 mg/mL; Zoetis Inc, Kalamazoo, Michigan).

2.5 | MRI protocol

Magnetic resonance imaging was performed using a 3T GE Discovery MR750 (GE Healthcare, Milwaukee, Wisconsin) whole body scanner (60 cm bore diameter), operating at 50 mT/m gradient amplitude and

TABLE 1 Each subject underwent a neurological examination and was neurologically graded according to this 5-stage, 15-point motor grading scale

Five-stage motor grading scale

Stage 1

- 0 Normal pelvic limb gait
- 1 Ataxic pelvic limb gait with normal strength, but mistakes made <50% of the time
- 2 Ataxic pelvic limb gait with normal strength, but mistakes >50% of the time (lack of coordination with thoracic limb, crossing of pelvic limbs, bunny hopping, scuffing foot on protraction)

Stage 2

- 3 Weight bearing protraction of pelvic limb 100% of the time with reduced strength. Mistakes <50% of the time
- 4 Weight bearing protraction of pelvic limbs 100% of the time with reduced strength. Mistakes 50% to 90% of the time
- 5 Weight bearing protraction 100% of the time with reduced strength of pelvic limb. Mistakes >90% of the time (crossing of pelvic limbs, scuffing foot on protraction, standing on dorsum, etc)

Stage 3

- 6 Weight bearing protraction of the pelvic limb >50% of the time
- 7 Weight bearing protraction of the pelvic limb 10% to 50% of the time
- 8 Weight bearing protraction of the pelvic limb <10% of the time

Stage 4

- 9 Nonweight bearing protraction of the pelvic limb with >1 joint involved >50% of the time
- 10 Nonweight bearing protraction of the pelvic limb with >1 joint involved <50% of the time
- 11 Minimal nonweight bearing protraction of the pelvic limb (movement of 1 joint)

Stage 5

- 12 No pelvic limb movement but voluntary tail movement
- 13 No pelvic limb movement with deep nociception
- 14 No pelvic limb movement and absent deep nociception

Notes: All control subjects had a grade of 0. Within the DM cohort one dog was grade 3, seven were grade 5, one was grade 8 and five were grade 9.

200 T/m/s slew rate. Subjects were placed in dorsal recumbency with the spine centered on a 12-channel spine coil. For structural evaluation of the vertebral column and slice placement guidance, a sagittal T2-weighted (TR 2700 ms, TE 103 ms, flip angle 142°, NEX 2, slice thickness 2 mm, matrix size 512 × 512, FOV 190 mm × 190 mm) sequence was performed. Transverse high-resolution proton density and diffusion tensor sequences were set up with matching orientation and location. Proton density scans (TR 4109 ms, TE 30 ms, flip angle 142°, slice thickness 5 mm, matrix 512 × 512, FOV 96 mm × 96 mm) were used to provide a structural reference for region of interest (ROI) analysis. The diffusion tensor sequence used a small field-of-

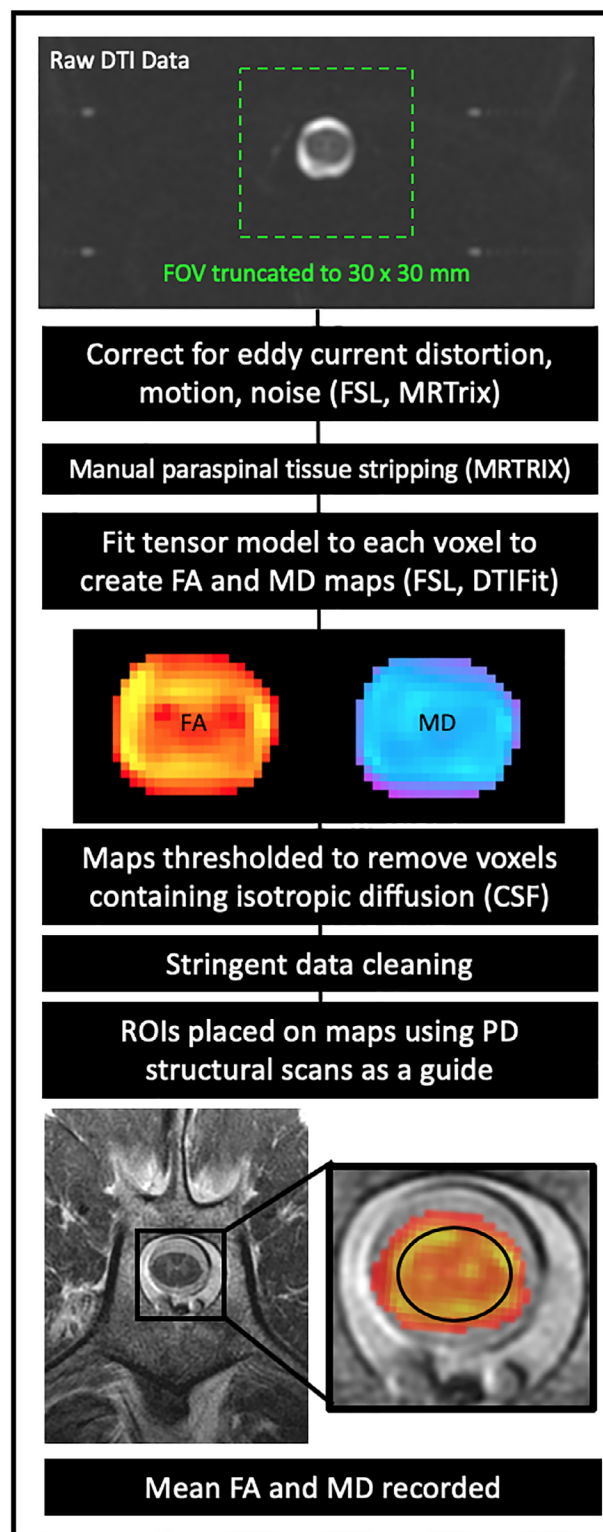


FIGURE 1 Flow chart diagram demonstrating the data processing methodology. Diffusion tensor imaging (DTI), field of view (FOV), cerebrospinal fluid (CSF), proton density (PD), fractional anisotropy (FA), mean diffusivity (MD)

view technique (FOV 48 mm × 96 mm) and was run with 9 directions. A nonisometric voxel was used (voxel size 1 × 1 × 5 mm³) to allow for whole spine scanning within a feasible time frame. Other parameters

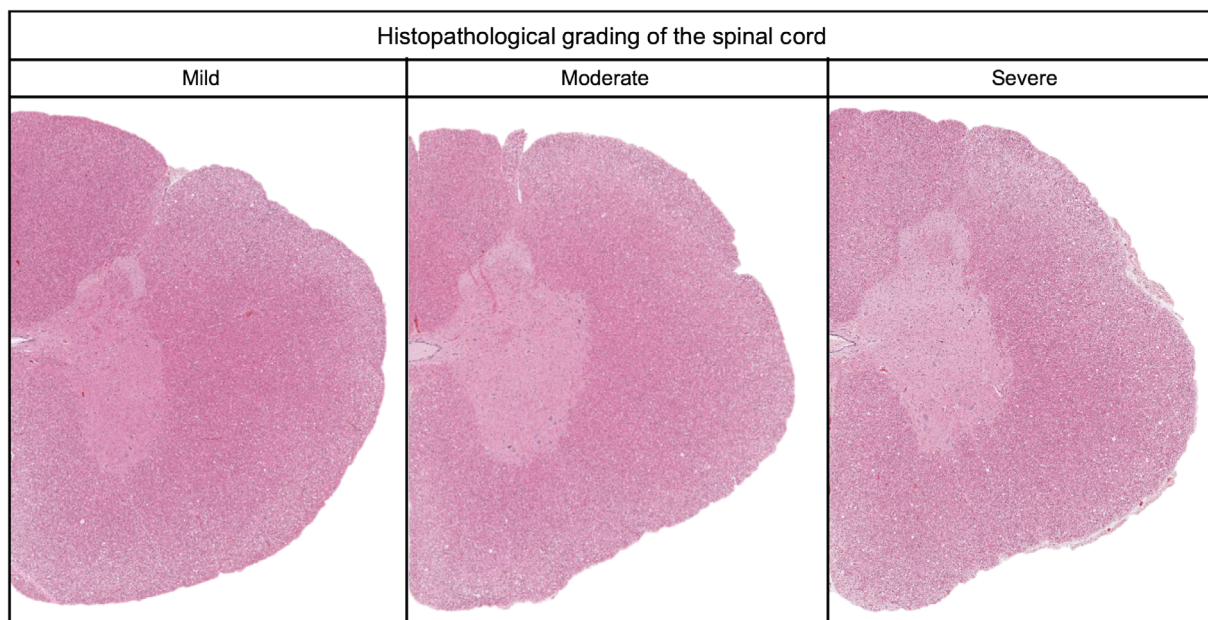


FIGURE 2 Transverse spinal cord slices that demonstrate mild, moderate and severe histopathological grades of lesion load

were as follows: B-value 800, TE 101.2 ms, TR 8305 ms, flip angle 90°, NEX 9, scan time 10 minutes 11 seconds to 14 minutes 48 seconds. Total scan time ranged from 1 hour 20 minutes to 2 hours 11 minutes depending on subject size.

2.6 | Structural imaging evaluation

For each subject, the T2-weighted and proton density sequences were evaluated by a specialist radiologist (P.J.J.) with advanced training in neuroimaging. The entire vertebral column was evaluated for concomitant pathology that may be contributing to the clinical presentation, including primary spinal cord lesions and sites of extradural spinal cord compression. If a clinically relevant lesion was identified, the subject was excluded. Sites of intervertebral disc protrusion without evidence of spinal cord compression were not considered clinically relevant.

2.7 | Data processing

Data were converted from Digital Imaging and Communications in Medicine (DICOM) to Neuroimaging Informatics Technology Initiative (NIFTI) format and underwent truncation of the field of view to 30 mm × 30 mm to focus on the spinal cord and remove peripheral noise. The data were then denoised using the *dwdenoise* command from MRtrix3²² software which uses principal component analysis (PCA) to identify data redundancy and estimate noise maps.^{23,24} Robust motion correction then was applied to the data using the *sct_dmri_moco* command from the Spinal Cord Toolbox²⁵ which uses a Gaussian mask, outlier detection, and regularization to register the 2D

slices in a group-wise fashion. The data then were corrected for eddy current distortion and inhomogeneity distortion using MRtrix's *dwiextract* command which functions as a command wrapper for FMRIB's Software Library (FSL) *eddy* and *topup* commands.²⁶⁻²⁸ Diffusion tensor FA and MD maps were generated for each slice by the standard ball-and-stick method using the *dtifit* command from FSL's FMRIB Diffusion Toolkit (FDT).^{29,30}

2.8 | Data cleaning

The FA diffusion tensor map then was used for quality control and data cleaning. Slices with obvious distortions, such as artificial geometric warping, or that had diffusivity measures outside of normal physiological means were marked and removed before statistical analysis. After this stringent data cleaning, approximately 30% of cervical slices, 64% of thoracic slices and 41% of lumbar slices had been excluded across participants. The remaining FA maps then were masked to a lower threshold of 0.2 and upper threshold of 0.9 to exclude voxels that contained signal from cerebrospinal fluid and ensure that retained voxels were within the normal physiological range. The created masks were applied to both FA and MD maps.

2.9 | Region of interest analysis

The ROI analysis was performed at midvertebral level to minimize the impact of spinal cord changes caused by chronic intervertebral disc disease. The mid-vertebral level single slice for each spinal section in each participant was defined by an experienced radiologist (P.J.J.). The ROIs were manually defined for each slice by an experienced analyst

Metric	Control		Mild DM		Severe DM		
	Mean	SD	Mean	SD	Mean	SD	
Cranial cervical							
C2	FA	0.518	0.061	0.487	0.069	0.492	0.032
	MD (mm ² /s)	0.00054	0.00017	0.00058	0.00020	0.00051	0.00021
C3	FA	0.571	0.037	0.551	0.031	0.54	0.031
	MD (mm ² /s)	0.00069	0.00015	0.00059	0.00013	0.00050	0.00008
Caudal cervical							
C4	FA	0.564	0.036	0.514	0.073	0.549	0.026
	MD (mm ² /s)	0.00077	0.00014	0.00075	0.00022	0.00061	0.00012
C5	FA	0.574	0.036	0.543	0.04	0.513	0.06
	MD (mm ² /s)	0.00088	0.00012	0.00062	0.00025	0.00067	0.00009
C6	FA	0.549	0.039	0.554	0.015	0.458	0.066
	MD (mm ² /s)	0.00083	0.00011	0.00066	0.00004	0.00086	0.00019
Midthoracic							
T5	FA	0.526	0.075	0.475	0.08	0.399	0.037
	MD (mm ² /s)	0.00062	0.00028	0.00057	0.00022	0.00085	0.00013
T6	FA	0.473	0.071	0.459	0.105	0.346	0.037
	MD (mm ² /s)	0.00078	0.00028	0.00057	0.00031	0.00080	0.00010
T7	FA	0.494	0.07	0.477	0.056	0.432	0.057
	MD (mm ² /s)	0.00057	0.00028	0.00052	0.00026	0.00057	0.00017
T8	FA	0.494	0.066	0.475	0.08	0.452	0.042
	MD (mm ² /s)	0.00054	0.00020	0.00045	0.00024	0.00049	0.00002
Cranial lumbar							
L2	FA	0.469	0.085	0.345	0.068	0.307	0.02
	MD (mm ² /s)	0.00079	0.00014	0.00077	0.00025	0.00088	0.00021
L3	FA	0.522	0.059	0.402	0.056	0.41	0.016
	MD (mm ² /s)	0.00087	0.00022	0.00074	0.00008	0.00081	0.00014
Caudal lumbar							
L4	FA	0.499	0.088	0.46	0.075	0.453	0.046
	MD (mm ² /s)	0.00092	0.00016	0.00073	0.00010	0.00073	0.00019
L5	FA	0.493	0.082	0.495	0.046	0.522	0.038
	MD (mm ² /s)	0.00100	0.00023	0.00070	0.00027	0.00078	0.00013

TABLE 2 Mean and SD for FA and MD values obtained from each tested segment of the spinal cord at the midvertebral body level for control (n = 13), mild degenerative myelopathy (DM) (n = 8), and severe DM groups (n = 6)

(E.F.B.) to include the entire cross section of the cord. Care was taken to ensure that voxels on the periphery of the spinal cord that may include signal from cerebrospinal fluid were avoided. For each ROI, the mean FA and MD from the included voxels was recorded. A flow chart for data processing, data cleaning and ROI analysis are presented in Figure 1.

2.10 | Pathology

Lesion grading was performed on a subset of dogs that underwent owner-elected euthanasia with necropsy and histopathology of the spinal cord within 3 weeks of imaging. The short time frame between imaging and necropsy ensured that lesion grading correlated as closely as possible with

the lesion status of the spinal cord at imaging. Spinal cord segments were subjectively graded according to lesion load on histopathology. Lesions were identified as axonal swelling with dilatation of the myelin sheath, and fragmentation and phagocytosis of myelin debris (ie, digestion chambers). Evaluated segments were graded as mild when lesions were present in <25% of the funiculi, moderate when lesions were present in 25% to 50% of the funiculi and severe when lesions were present in >50% of the funiculi (Figure 2). This information was used to confirm the pattern of lesion severity throughout 7 defined segments of the spinal cord: cranial cervical (C2-4), caudal cervical (C5-8), cranial thoracic (T1-4), midthoracic (T5-9), caudal thoracic (T10-13), cranial lumbar (L1-3) and caudal lumbar (L4-5). In addition, the FA and MD parameters at each spinal cord level were plotted against lesion grade, allowing a direct comparison between histopathological grading and imaging results.

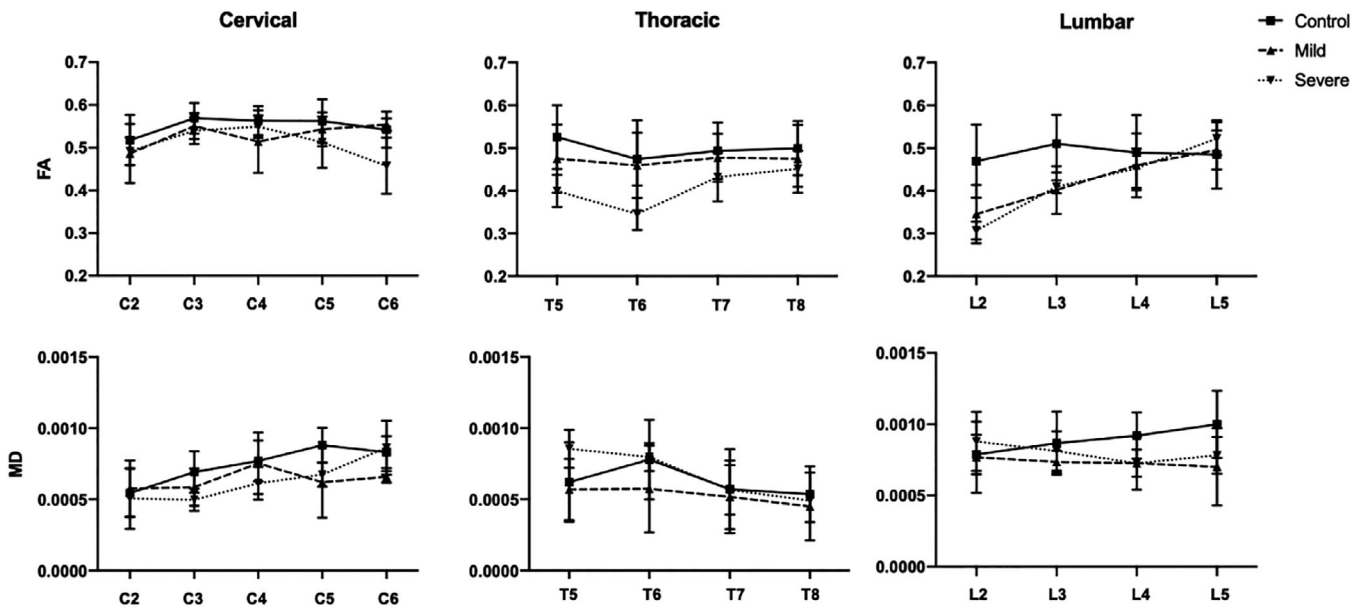


FIGURE 3 Charts documenting the mean fractional anisotropy (FA) and mean diffusivity (MD) (mm^2/s) values obtained at each midvertebral segment along the analyzed spinal cord for the control (solid black line), mild degenerative myelopathy (DM) (dashed black line) and severe DM (dotted black line)

2.11 | Statistical analysis

To visually demonstrate the pattern of FA and MD alterations at each midvertebral level throughout the analyzed spinal cord for the control, mild DM and severe DM groups data were documented and plotted. Because of substantial data loss at the C7-T4 and T9-L1 levels arising from data cleaning, these regions were excluded from all analyses.

Data were normally distributed based on Kolmogorov-Smirnov testing. Preliminary analysis aimed to identify if the tested metrics (FA and MD) showed significant differences in the cranial cervical (C2-3), caudal cervical (C4-6), midthoracic (T5-8), cranial lumbar (L2-3), and caudal lumbar regions (L4-5) between DM and control groups. For each region the FA and MD data from included slices were averaged for each subject. A 2-tailed Student's *t*-test determined the presence of statistically significant differences between DM and control groups for each evaluated spinal segment ($P < .05$ established statistical significance). To evaluate the effect of neurological group (control, mild and severe) on DTI measures, the data were analyzed using a 1-way analysis of variance (ANOVA) to identify statistically significant differences between groups. At sites where significance was identified, a post hoc Dunnett's method test was performed to compare the mild and severe groups with the control group. To assess whether diffusivity alterations correlated with neurological decline, a Spearman's rank correlation coefficient was used to identify correlations between diffusivity parameters and neurological grade.

3 | RESULTS

3.1 | Degenerative myelopathy cohort

Fourteen dogs met the inclusion criteria for the DM cohort. Twelve dogs were euthanized at the owners' request and underwent

necropsy with histopathology of the spinal cord; 11 dogs were confirmed with DM and 1 dog had an indeterminate diagnosis because of the presence of a concurrent vertebral stenosis and was excluded from the study. Two dogs still were alive at the time of manuscript preparation and were included in the study. The signalment and neurological grade for each included dog is provided in the Supporting Information. This cohort had a median age of 9 years (range, 6-13 years) and a median weight of 31 kg (range, 9-39 kg).

3.2 | Control cohort

Thirteen dogs met the inclusion criteria for the control cohort. The signalment and neurological grade for each included dog is provided in the Supporting Information. This cohort had a median age of 10 years (range, 8-12 years) and a median weight of 21 kg (range, 7-31 kg).

3.3 | Descriptive statistics

The mean and standard deviation (SD) FA and MD (mm^2/s) results for the control, mild DM and severe DM groups are provided in Table 2. The FA and MD results obtained at each midvertebral level from control, mild DM, and severe DM groups are plotted for the cervical, thoracic, and lumbar regions in Figure 3.

3.4 | Differences in diffusivity parameters between control and DM cohorts

Two-tailed Student's *t*-tests comparing control and DM cohorts for each metric, identified statistically significant differences in FA in the caudal

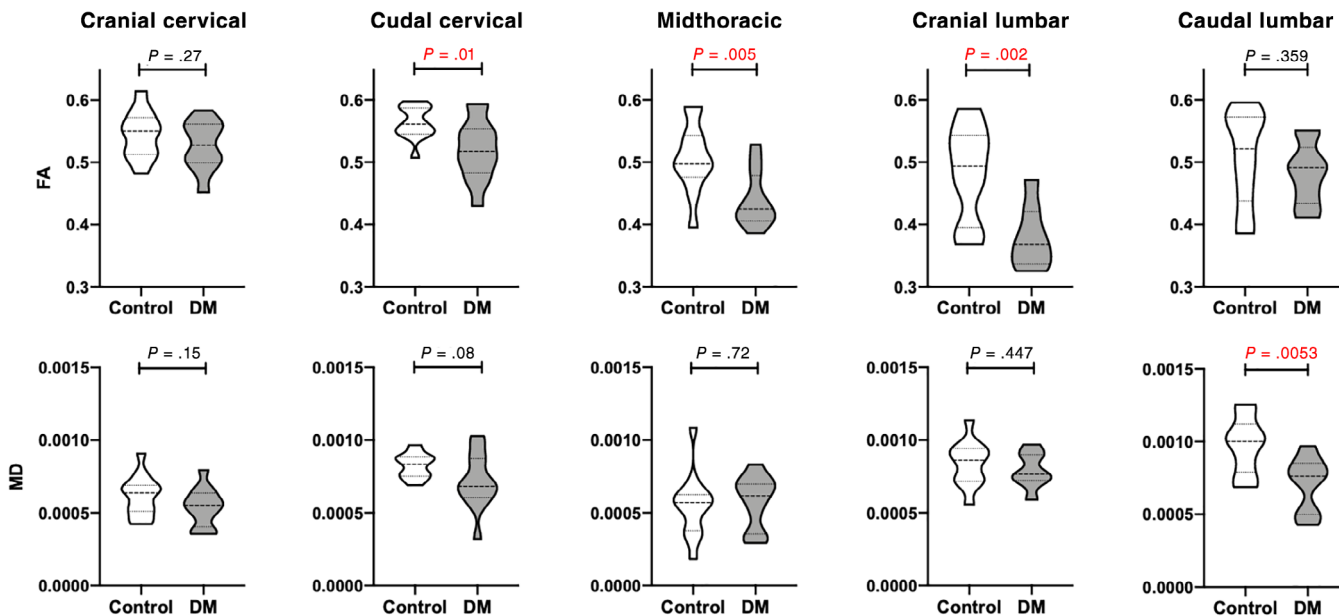


FIGURE 4 Violin plots demonstrating the fractional anisotropy (FA) and mean diffusivity (MD) (mm^2/s) for control and degenerative myelopathy (DM) cohorts and the results of the two-tailed student's *t*-test performed to compare between groups. Statistically significant difference ($P < .05$) is highlighted in red and was found for FA between groups at the caudal cervical, midthoracic and cranial lumbar levels

cervical ($P = .01$), midthoracic ($P = .005$) and cranial lumbar ($P = .002$) regions (Figure 4) and in MD (mm^2/s) in the caudal lumbar region ($P = .005$).

performed on the cranial lumbar region, it identified a statistically significant difference between control and mild groups ($P = .02$) only (Figure 5).

3.5 | Differences in diffusivity parameters between control and mild or severely affected cohorts

3.5.1 | Fractional anisotropy

One-way ANOVA performed among control, mild and severe groups identified statistically significant differences between groups within the caudal cervical region ($P = .03$), midthoracic ($P = .01$) and cranial lumbar ($P = .02$) regions. The 1-way ANOVA showed no significant differences in FA in the cranial cervical ($P = .49$) and caudal lumbar ($P = .64$) regions. When a Dunnett's test was performed on the regions that demonstrated significant differences, the severe DM group was identified as having a significantly different FA as compared with the control group in both the caudal cervical ($P = .03$) and the midthoracic regions ($P = .01$) and both the mild and severe DM groups had significantly different FA compared with the control group in the cranial lumbar region ($P = .03$ and $P = .05$, respectively; Figure 5).

3.5.2 | Mean diffusivity (mm^2/s)

The 1-way ANOVA only identified statistically significant differences between groups in the caudal lumbar region ($P = .02$) with all other regions not showing significant differences (cranial cervical region, $P = .23$; caudal cervical region, $P = .19$; midthoracic region, $P = .36$; and cranial lumbar region, $P = .46$). When a Dunnett's test was

3.6 | Correlations between neurological grade and diffusivity parameters

3.6.1 | Fractional anisotropy

Mean FA values showed moderate negative correlation with neurological grade in the caudal cervical ($r_s = -0.47$, $P = .02$), midthoracic ($r_s = -0.58$, $P = .003$) and cranial lumbar regions ($r_s = -0.60$, $P = .007$), but showed only weak negative correlation in the cranial cervical ($r_s = -0.18$, $P = .39$) and caudal lumbar ($r_s = -0.24$, $P = .29$) regions.

3.6.2 | Mean diffusivity (mm^2/s)

Mean MD values showed moderate negative correlations with neurological grade in the caudal cervical ($r_s = -0.480$, $P = .01$) and caudal lumbar ($r_s = -0.550$, $P = .008$) regions and showed weak correlations in the cranial cervical ($r_s = -0.342$, $P = .09$), mid thoracic ($r_s = 0.239$, $P = .26$), and cranial lumbar ($r_s = -0.060$, $P = 0.8$) regions.

3.7 | Histopathological lesion grading

Three of the 11 dogs that underwent necropsy and histopathology of the spinal cord met the timing requirements for inclusion into histopathological grading. The signalment, neurological grade, time from

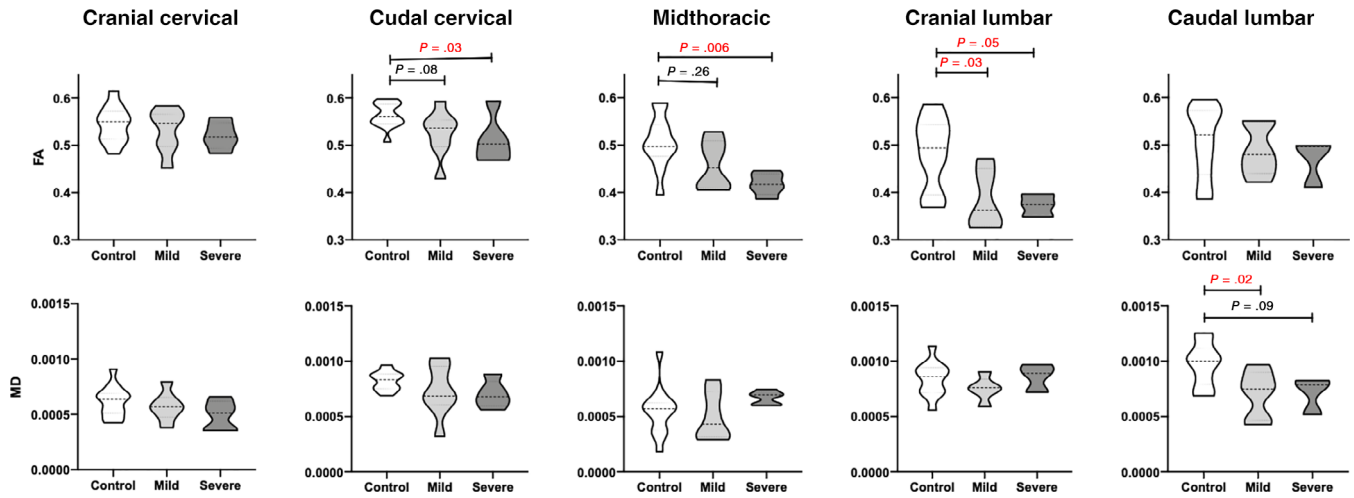


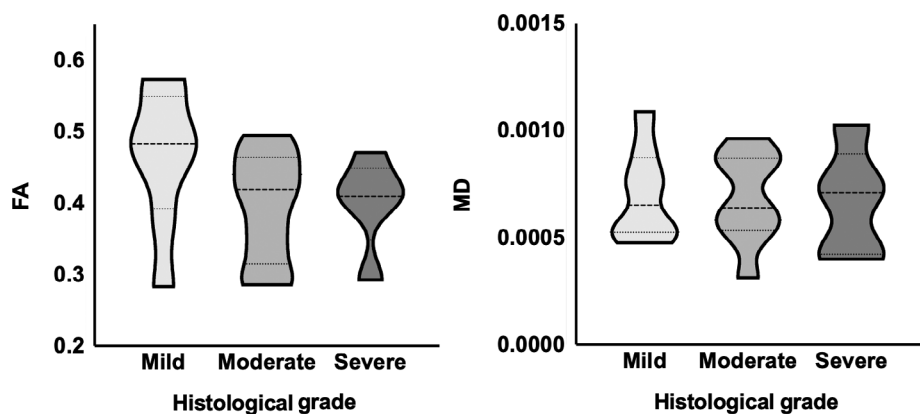
FIGURE 5 Violin plots demonstrating the fractional anisotropy (FA) and mean diffusivity (MD) (mm^2/s) for control, mild degenerative myelopathy (DM) and severe DM cohorts. A 1-way ANOVA with a post hoc Dunnett's test was used to identify statistically significant difference between groups. Statistically significant difference ($P < .05$) is highlighted in red. FA: At the caudal cervical and midthoracic regions, the severe group was statistically lower to the control group, whereas at the cranial lumbar region both mild and severe DM groups were statistically lower to controls. MD: Within the caudal lumbar region MD was statistically lower in the mild DM group when compared to the control group

TABLE 3 Signalment, neurological grade, time interval between magnetic resonance imaging (MRI), and postmortem (PM) and histological grading results for a subgroup of degenerative myelopathy dogs

		1	2	3
Signalment	Breed	Mixed	Corgi	GSD
	Sex	Fs	Mn	Fs
	Age (y)	6	10	9
	Neurological grade	5	8	9
	MRI to PM interval	4 d	1 d	21 d
Histological grading	Cranial cervical (C2-4)	Mild	Mild	Mild
	Caudal cervical (C5-8)	Mild	Mild	Moderate
	Cranial thoracic (T1-4)	Moderate	Mild	Moderate
	Mid thoracic (T5-9)	Moderate	Moderate	Severe
	Caudal thoracic (T10-13)	Moderate	Moderate	Severe
	Cranial lumbar (L1-3)	Moderate	Severe	Severe
	Caudal lumbar (L4-5)	Moderate	NS	Moderate

Abbreviations: FS, female spayed; GSD, German shepherd dog; MN, male neutered; NS, not sampled.

FIGURE 6 Violin plots documenting the fractional anisotropy (FA) and mean diffusivity (MD) (mm^2/s) found at sites graded on histopathology as mild, moderate, and severe. Although there is overlap between the groups, the mean FA for the mild sites is higher than that of the moderate and severe sites



imaging to histopathological evaluation and histopathological grade are presented in Table 3. All spinal cords had the most marked lesion loads in the thoracic and cranial lumbar regions. When diffusivity values were compared to histopathological grade, measured mean FA was higher for sites with mild lesions (0.46 ± 0.09) when compared to sites with moderate (0.39 ± 0.07) or severe (0.4 ± 0.06) lesions, and mean MD values were similar for all grades: mild (0.00069 ± 0.00022), moderate (0.00069 ± 0.00021) and severe (0.00067 ± 0.00025). These data are plotted for each grade (mild, moderate, and severe) in Figure 6.

4 | DISCUSSION

These data support the tested hypotheses and identified that at spinal cord sites where lesion load was expected to be the highest, FA was significantly decreased in the DM cohort. These changes were most notable in dogs with severe forms of DM and were negatively correlated with neurological grade, suggesting that this metric has potential to be used as a clinical biomarker for the disease.

Degenerative myelopathy causes segmental degeneration of the axon and associated myelin within the spinal cord of dogs.³ At necropsy, a pattern of lesion development is observed with lesions being more severe within the thoracic region, where they originate, and progressively less severe in the cervical and lumbar regions on histopathology.^{31,32} In our study, this pattern of lesion load was observed in the subgroup of dogs that were histopathologically graded, with all 3 subjects exhibiting their most severe lesions in the midthoracic, caudal thoracic or cranial lumbar regions and exhibiting milder lesions in the cranial cervical and caudal lumbar regions. Understanding the expected pattern of spinal cord lesions in the cohort of clinical DM subjects helped us interpret our DTI results. We identified significantly decreased FA values in the midthoracic, caudal cervical and cranial lumbar subregions, which is consistent with the pattern of expected lesion load. In the cranial cervical and caudal lumbar regions, where lesions are expected to be milder until the disease has reached an advanced stage, FA values were not statistically different from those of the control cohort. On the other hand, MD did not show alterations that matched expected lesion load, only showing statistically significant alterations in the caudal lumbar region. The pattern of FA alterations corroborates expected lesion load and therefore our findings support FA as a potential clinical tool in DM diagnosis and monitoring.

On statistical evaluation of spinal cord sites where lesions were most severe, significant alterations were only identified in FA and not in MD. This finding is consistent with that observed in several ALS studies of humans that evaluated the spinal cord and identified significant FA decreases but no significant MD alterations.^{9,33,34} Neuropathology can cause variable alterations in MD with different components of complex diseases causing opposing factors that result in unpredictable results. For example inflammation and an increase in tissue water can cause MD increases and cell proliferation can cause MD decreases.³⁵ For these reasons, MD may be insensitive to the presence of certain complex lesions, which could indicate why no

statistically significant alterations in MD were found in high lesion load regions and a significant decrease in MD was found in a region where we would not expect lesions within our DM cohort.

Identifying the relationship of DTI metrics to neurological outcome measures helps explore the utility of in vivo imaging for monitoring lesion load, as shown with our findings in a DM canine population and provides support for the use of DTI metrics as potential clinical biomarkers in DM and other conditions.^{10,36} In human disease, FA is a promising biomarker for disability in numerous spinal cord pathologies.¹⁰ Studies of ALS have consistently identified relationships between FA and functional outcome measures, including the ALS functional rating scale, with correlations ranging from moderate to strong.^{9,33,34,37,38} In our study, we identified that in subregions of the spinal cord where lesions were expected to be most severe, a moderate to strong correlation existed between FA and neurological grade. These findings suggest that FA has the potential to act as an MRI biomarker for neurological disability in DM.

In the 3 dogs that underwent owner-elected euthanasia and necropsy, within 3 weeks of imaging, we directly compared our FA and MD values to histopathological grade of the spinal cord. The case numbers were too low for statistical evaluation, but on subjective evaluation FA decreased with more severe lesions whereas the MD results remained similar across groups. Direct spinal cord histopathological correlation with in vivo DTI metrics has previously only been performed in rodent models of ALS and has never been described in studies of spontaneous ALS in humans.^{39,40} Our study is the first to directly compare histopathology with DTI metrics in a spontaneous ALS model and provides preliminary evidence for future research to validate these methods.

Diffusion tensor imaging is an advanced MRI technique that increasingly has been incorporated into clinical evaluations of humans with neurological disease.⁴¹ It can be performed on either 1.5-Tesla or 3.0-Tesla systems, both of which are available in academic and larger referral veterinary hospitals, and several academic centers have already started applying it in spinal cord research in dogs.^{17,18,42} The transition of spinal cord DTI from the research setting to clinical setting for diagnostic, prognostic and longitudinal monitoring purposes would require assessment of the sensitivity and specificity of DTI for detecting lesions in single subjects. Doing so would require development of normal thresholds, and future studies with larger cohorts of dogs with DM could further develop these standards. In addition, although FA metrics are sensitive to spinal cord lesions, they are not specific, and understanding how the pattern, distribution and severity of spinal cord FA changes are altered by other spinal cord disease processes, such as intervertebral disc disease, in comparison with DM will help to determine whether this method is capable of differentiating among different pathologies.

A limitation of spinal cord DTI is that it often is impacted by low signal and artifacts.⁴³ We designed our protocols using previously published descriptions of spinal DTI in dogs^{15,17} and applied a small field-of-view technique to minimize the impact of motion and magnetic field inhomogeneity.^{44,45} Despite these sequence optimization and postprocessing measures, data cleaning resulted in substantial loss of data at the cervicothoracic and thoracolumbar junction regions. At the

cervicothoracic level, the loss of data was mostly a result of low signal and high levels of noise, likely caused by increased distance of the spinal cord from the surface coil used.⁴³ This effect may have been decreased by using with a different coil combination or with altered coil placement. At the thoracolumbar junction level, data loss occurred secondary to substantial cardiovascular and respiratory motion artifact, magnetic field inhomogeneity and wrap-around. These effects are likely caused by the close proximity of the pulsating aorta and lung-bone interface to the thoracolumbar spinal cord, causing off-resonance artifacts, susceptibility signal drop-out and anatomic distortions.⁴³ These artifacts potentially may have been minimized if cardiac or respiratory gating techniques had been used, but with our system, gating would not allow for DTI acquisition within a reasonable time frame. With continual improvement in DTI and MRI technology, the impact of artifacts and noise on DTI data is likely to be decreased. Our sequence protocol also utilized a nonisometric voxel size (1 × 1 × 5 mm). This allowed us to have a high in-plane resolution without low signal, and is a common method used in spinal DTI.^{15,17} However, this method comes with limitations because nonisometric voxels introduce bias in the quantitative assessment of fiber orientation and anisotropy.^{46,47} Future research is needed to optimize DTI protocols for the canine population and for challenges specific to spinal cord imaging.

In our study the disease cohort was relatively small and included dogs of variable breeds and sizes. Increasing subject numbers would improve statistical power and potentially provide more information on the diffusivity alterations observed in dogs at different stages of the condition. In addition, focused breed-specific studies would help limit breed-related variability and assist in identifying differences across breeds in DM.

We evaluated the diffusivity parameters FA and MD, but DTI data can provide other measures of diffusivity, including radial diffusivity (RD) and axial diffusivity (AD).⁴⁸ These measures provide information on different aspects of diffusion, with RD relating to myelination, axon diameters and density and AD relating to axonal injury and disease.^{14,49} Although these parameters have been shown to be altered with neuropathology, including ALS lesions,⁸ FA and MD have the most consistent alterations secondary to neuropathology in the spinal cord.¹⁰ Therefore, to minimize the issue of multiple comparisons, FA and MD were chosen for our analyses. Future studies could consider evaluating the effect of DM spinal cord lesions on other diffusivity parameters. Other MRI parameters that could be considered in future MRI evaluations of DM include assessment of spinal cord volume change. Dogs with DM have smaller spinal cords than healthy dogs,⁵⁰ and volume metrics could be integrated into the MRI evaluation of the spinal cord to provide a multimodal evaluation of the changes observed.

We found that in dogs with DM, DTI MRI can identify significant decreases in FA within the regions of the spinal cord that are expected to have moderate to severe lesion load. In addition, FA alterations were related to the neurological status of subjects and showed a negative trend with respect to histopathological grading of lesions. These findings suggest that FA has the potential to be a biomarker for spinal cord lesion development in DM and with further validation, could play an important role in improving diagnosis and monitoring of this condition.

ACKNOWLEDGMENTS

Funding provided by Morris Animal Foundation, grant D18CA-310. We thank the Vaika Foundation for providing subjects for the control cohort. We acknowledge Dr Mathew Brunke for assisting with recruitment.

CONFLICT OF INTEREST DECLARATION

Authors declare no conflict of interest.

OFF-LABEL ANTIMICROBIAL DECLARATION

Authors declare no off-label use of antimicrobials.

INSTITUTIONAL ANIMAL CARE AND USE COMMITTEE (IACUC) OR OTHER APPROVAL DECLARATION

Approved by the Cornell University Animal Care and Use Committee, protocols 2015-0115 and 2016-0021.

HUMAN ETHICS APPROVAL DECLARATION

Authors declare human ethics approval was not needed for this study.

ORCID

Philippa J. Johnson  <https://orcid.org/0000-0002-4558-0745>

John P. Loftus  <https://orcid.org/0000-0001-7181-7155>

REFERENCES

- Zeng R, Coates JR, Johnson GC, et al. Breed distribution of SOD1 alleles previously associated with canine degenerative myelopathy. *J Vet Intern Med.* 2014;28(2):515-521.
- Kathmann I, Cizinauskas S, Doherr MG, Steffen F, Jaggy A. Daily controlled physiotherapy increases survival time in dogs with suspected degenerative myelopathy. *J Vet Intern Med.* 2006;20(4):927-932.
- Coates JR, Winiinger FA. Canine degenerative myelopathy. *Vet Clin North Am Small Anim Pract.* 2010;40(5):929-950.
- Capucchio MT, Spalenza V, Biasibetti E, et al. Degenerative myelopathy in German shepherd dog: comparison of two molecular assays for the identification of the SOD1:c.118G>A mutation. *Mol Biol Rep.* 2014;41:665-670.
- Holder AL, Price JA, Adams JP, Volk HA, Catchpole B. A retrospective study of the prevalence of the canine degenerative myelopathy associated superoxide dismutase 1 mutation (SOD1:c.118G>A) in a referral population of German shepherd dogs from the UK. *Canine Genet Epidemiol.* 2014;1:10.
- Kobatake Y, Sakai H, Tsukui T, et al. Localization of a mutant SOD1 protein in E40K-heterozygous dogs: implications for non-cell-autonomous pathogenesis of degenerative myelopathy. *J Neurol Sci.* 2017;372:369-378.
- Nardone R, Höller Y, Taylor AC, et al. Canine degenerative myelopathy: a model of human amyotrophic lateral sclerosis. *Fortschr Zool.* 2016;119:64-73.
- Foerster BR, Dwamena BA, Petrou M, et al. Diagnostic accuracy of diffusion tensor imaging in amyotrophic lateral sclerosis: a systematic review and individual patient data meta-analysis. *Acad Radiol.* 2013;20(9):1099-1106.
- Nair G, Carew JD, Usher S, Lu D, Hu XP, Benatar M. Diffusion tensor imaging reveals regional differences in the cervical spinal cord in amyotrophic lateral sclerosis. *Neuroimage.* 2010;53(2):576-583.
- Martin AR, Aleksanderek I, Cohen-Adad J, et al. Translating state-of-the-art spinal cord MRI techniques to clinical use: a systematic review of clinical studies utilizing DTI, MT, MWF, MRS, and fMRI. *Neuroimage Clin.* 2016;10:192-238.
- Basser PJ, Pierpaoli C. Microstructural and physiological features of tissues elucidated by quantitative-diffusion-tensor MRI. *J Magn Reson Ser B.* 1996;111:209-219.

12. Wheeler-Kingshott CAM, Hickman SJ, Parker GJM, et al. Investigating cervical spinal cord structure using axial diffusion tensor imaging. *Neuroimage*. 2002;16(1):93-102.
13. Basser PJ, Mattiello J, LeBihan D. MR diffusion tensor spectroscopy and imaging. *Biophys J*. 1994;66(1):259-267.
14. Johansen-Berg H, Behrens TEJ. Introduction to diffusion MRI. Section III. Diffusion in neural tissue. *Diffusion MRI: From Quantitative Measurement to in vivo Neuroanatomy*. 2nd ed.; Elsevier, Academic Press Inc: Cambridge, MA, USA. 2013:8-10.
15. Griffin JF, Cohen ND, Young BD, et al. Thoracic and lumbar spinal cord diffusion tensor imaging in dogs. *J Magn Reson Imaging*. 2013;37(3):632-641.
16. Vedantam A, Jirjis MB, Schmit BD, Wang MC, Ulmer JL, Kurpad SN. Diffusion tensor imaging of the spinal cord: insights from animal and human studies. *Neurosurgery*. 2014;74:1-8.
17. Yoon H, won PN, Ha YM, Kim J, Moon WJ, Eom K. Diffusion tensor imaging of white and grey matter within the spinal cord of normal Beagle dogs: sub-regional differences of the various diffusion parameters. *Vet J*. 2016;215:110-117.
18. Lewis MJ, Yap PT, McCullough S, Olby NJ. The relationship between lesion severity characterized by diffusion tensor imaging and motor function in chronic canine spinal cord injury. *J Neurotrauma*. 2018;35(3):500-507.
19. Liu C, Yang D, Li J, et al. Dynamic diffusion tensor imaging of spinal cord contusion: a canine model. *J Neurosci Res*. 2018;96(6):1093-1103.
20. Loy DN, Joong HK, Xie M, Schmidt RE, Trinkaus K, Song SKV. Diffusion tensor imaging predicts hyperacute spinal cord injury severity. *J Neurotrauma*. 2007;24(6):979-990.
21. Olby NJ, De Risio L, Muñana KR, et al. Development of a functional scoring system in dogs with acute spinal cord injuries. *Am J Vet Res*. 2001;62(10):1624-1628.
22. Tournier JD, Smith R, Raffelt D, et al. MRtrix3: a fast, flexible and open software framework for medical image processing and visualisation. *Neuroimage*. 2019;202:116137.
23. Veraart J, Fieremans E, Novikov DS. Diffusion MRI noise mapping using random matrix theory. *Magn Reson Med*. 2016;76(5):1582-1593.
24. Veraart J, Novikov DS, Christiaens D, Ades-aron B, Sijbers J, Fieremans E. Denoising of diffusion MRI using random matrix theory. *Neuroimage*. 2016;142:394-406.
25. De Leener B, Lévy S, Dupont SM, et al. SCT: spinal cord toolbox, an open-source software for processing spinal cord MRI data. *Neuroimage*. 2017;145:24-43.
26. Andersson JLR, Sotiropoulos SN. An integrated approach to correction for off-resonance effects and subject movement in diffusion MR imaging. *Neuroimage*. 2016;125:1063-1078.
27. Smith SM, Jenkinson M, Woolrich MW, et al. Advances in functional and structural MR image analysis and implementation as FSL. *Neuroimage*. 2004;23:S208-S219.
28. Andersson JLR, Skare S, Ashburner J. How to correct susceptibility distortions in spin-echo echo-planar images: application to diffusion tensor imaging. *Neuroimage*. 2003;20(2):870-888.
29. Behrens TEJ, Woolrich MW, Jenkinson M, et al. Characterization and propagation of uncertainty in diffusion-weighted MR imaging. *Magn Reson Med*. 2003;50(5):1077-1088.
30. Behrens TEJ, Berg HJ, Jbabdi S, Rushworth MFS, Woolrich MW. Probabilistic diffusion tractography with multiple fibre orientations: what can we gain? *Neuroimage*. 2007;34(1):144-155.
31. Averill DR. Degenerative myelopathy in the aging German shepherd dog: clinical and pathologic findings. *J Am Vet Med Assoc*. 1973;162(12):1045-1051.
32. March PA, Coates JR, Abyad RJ, et al. Degenerative myelopathy in 18 Pembroke welsh corgi dogs. *Vet Pathol*. 2009;46(2):241-250.
33. Valsasina P, Agosta F, Benedetti B, et al. Diffusion anisotropy of the cervical cord is strictly associated with disability in amyotrophic lateral sclerosis. *J Neurol Neurosurg Psychiatry*. 2007;78(5):480-484.
34. Cohen-Adad J, El MM-M, Morizot-Koutlidis R, et al. Involvement of spinal sensory pathway in ALS and specificity of cord atrophy to lower motor neuron degeneration. *Amyotroph Lateral Scler Front Degener*. 2013;14(1):30-38.
35. Alexander AL, Lee JE, Lazar M, Field AS. Diffusion tensor imaging of the brain. *Neurotherapeutics*. 2007;4(3):316-329.
36. Strimbu K, Tavel JA. What are biomarkers? *Curr Opin HIV AIDS*. 2010;5:463-466.
37. Agosta F, Rocca MA, Valsasina P, et al. A longitudinal diffusion tensor MRI study of the cervical cord and brain in amyotrophic lateral sclerosis patients. *J Neurol Neurosurg Psychiatry*. 2009;80(1):53-55.
38. El Mendili MM, Cohen-Adad J, Pelegrini-Issac M, et al. Multi-parametric spinal cord MRI as potential progression marker in amyotrophic lateral sclerosis. *PLoS One*. 2014;9(4):e95516.
39. Gatto RG, Amin MY, Deyoung D, Hey M, Mareci TH, Magin RL. Ultra-high field diffusion MRI reveals early axonal pathology in spinal cord of ALS mice. *Transl Neurodegener*. 2018;7(1):20.
40. Underwood CK, Kurniawan ND, Butler TJ, Cowin GJ, Wallace RH. Non-invasive diffusion tensor imaging detects white matter degeneration in the spinal cord of a mouse model of amyotrophic lateral sclerosis. *Neuroimage*. 2011;55(2):455-461.
41. Tae WS, Ham BJ, Pyun SB, Kang SH, Kim BJ. Current clinical applications of diffusion-tensor imaging in neurological disorders. *J Clin Neurol*. 2018;14:129-140.
42. Hobert MK, Stein VM, Dziallas P, Ludwig DC, Tipold A. Evaluation of normal appearing spinal cord by diffusion tensor imaging, fiber tracking, fractional anisotropy, and apparent diffusion coefficient measurement in 13 dogs. *Acta Vet Scand*. 2013;55:36.
43. Rutman AM, Peterson DJ, Cohen WA, Mossa-Basha M. Diffusion tensor imaging of the spinal cord: clinical value, investigational applications, and technical limitations. *Curr Prob Diagn Radiol*. 2018;47:257-269.
44. Tang L, Wen Y, Zhou Z, von Deneen KM, Huang D, Ma L. Reduced field-of-view DTI segmentation of cervical spine tissue. *Magn Reson Imaging*. 2013;31(9):1507-1514.
45. Yokohama T, Iwasaki M, Oura D, Furuya S, Okuaki T. The reliability of reduced field-of-view DTI for highly accurate quantitative assessment of cervical spinal cord tracts. *Magn Reson Med Sci*. 2019;18(1):36-43.
46. Soares JM, Marques P, Alves V, Sousa N. A hitchhiker's guide to diffusion tensor imaging. *Front Neurosci*. 2013;7(7):31.
47. Mukherjee P, Chung SW, Berman JI, Hess CP, Henry RG. Diffusion tensor MR imaging and fiber tractography: technical considerations. *Am J Neuroradiol*. 2008;29:843-852.
48. Jones DK. Gaussian modeling of the diffusion signal. *Diffusion MRI*. Elsevier, Academic Press Inc: Cambridge, MA, USA. 2014:87-104.
49. Westin C-F, Maier SE, Mamata H, Nabavi A, Jolesz FA, Kikinis R. Processing and visualization for diffusion tensor MRI. *Med Image Anal*. 2002;6(2):93-108.
50. Jones JC, Inzana KD, Rossmel JH, Bergman RL, Wells T, Butler K. CT myelography of the thoraco-lumbar spine in 8 dogs with degenerative myelopathy. *Comp Study*. 2005;6:341-348.

SUPPORTING INFORMATION

Additional supporting information may be found online in the Supporting Information section at the end of this article.

How to cite this article: Johnson PJ, Miller AD, Cheetham J, et al. In vivo detection of microstructural spinal cord lesions in dogs with degenerative myelopathy using diffusion tensor imaging. *J Vet Intern Med*. 2021;35:352-362. <https://doi.org/10.1111/jvim.16014>